Haptotropic Rearrangement between Two Isomers of (μ_2:η^3:η^5-guaiazulene)$Fe_2(CO)_5$ Revisited: Both Thermal and Photochemical Processes Induce the Haptotropic Interconversion

Hideo Nagashima,* Takahiko Fukahori, Mitsuharu Nobata, Akihiro Suzuki, Mitsuhiko Nakazawa, and Kenji Itoh

Department of Materials Science, Toyohashi University of Technology, Toyohashi, Aichi 441, Japan

Received December 7, 1993[⊗]

Interconversion between two haptotropic isomers of (μ_2:η^3:η^5-guaiazulene)$Fe_2(CO)_5$ (**1a,b**) occurred at 70–105 °C. The thermal equilibrium ratios between **1a** and **1b** are around 55:45 in this temperature range, indicating that **1a** is more stable than **1b** by 0.1 kcal/mol. The activation energies estimated from kinetic studies are $\Delta G^{\ddagger}_{373} = 28 \pm 1$ kcal/mol, $\Delta H^{\ddagger}_{373} = 23 \pm 2$ kcal/mol, and $\Delta S^{\ddagger}_{373} = -15 \pm 5$ cal/(mol·deg) either from **1a** to **1b** or from **1b** to **1a**. UV or visible photolysis also induced the interconversion to give a mixture of **1a,b** in a ratio of 35:65. The haptotropic rearrangement of the ruthenium analogues, (μ_2:η^3:η^5-guaiazulene)-$Ru_2(CO)_5$ (**2a,b**), also occurred either thermally or photochemically to give a mixture of isomers in a ratio of 55:45. Photochemical replacement of CO ligands in **1a,b** by PEt_3 gave a mixture of mono- and diphosphine compounds, (μ_2:η^3:η^5-guaiazulene)$Fe_2(PEt_3)(CO)_4$ (**4**) and (μ_2:η^3:η^5-guaiazulene)$Fe_2(PEt_3)_2(CO)_3$ (**5**), the ratio of which was controlled by the amount of added PEt_3. Mechanistic aspects are discussed on the basis of the reaction profile of the haptotropic interconversion and the ligand substitution.

Introduction

Migration of organometallic species among possible coordination sites of polyene or polyaromatic ligands is well-known as the haptotropic rearrangement, and many studies have been made with ligand dynamics and with MO calculations.[1,2] However, the possibility that the rearrangement could take place by a photochemical process has not been reported until our recent discovery that a symmetrical isomer of (μ_2:η^3:η^5-acenaphthylene)-$Fe_2(CO)_5$ (**3a**) is exclusively converted to a less thermodynamically stable unsymmetrical isomer (**3b**) under irradiation.[3] The fact that the reverse reaction from **3b** to **3a** occurred in the dark at room temperature showed that the switching of the coordination site of the acenaphthylene ligand on the $Fe_2(CO)_5$ species could be directed by either exposure or protection from the light. It is of interest to us whether this photoswitch-like behavior of the diiron complex can also be observed in other bimetallic compounds bound to polyaromatic or polyolefin ligands.[1]

Two isomers of (μ_2:η^3:η^5-guaiazulene)$Fe_2(CO)_5$ (**1a,b**) were reported by Cotton and co-workers and are a rare example where preparation, successful separation, and a crystal structure determination were carried out.[4a] Exchange processes of the carbonyl ligands in these compounds were extensively studied by the authors;[4a] however, the haptotropic rearrangement between **1a** and **1b** was obscure probably due to complicated and hardly assignable patterns of their ^1H NMR spectra.[4b] We carried out the unequivocal assignment of NMR spectra of **1a,b** and studied the thermal and photochemical haptotropic interconversions between them in detail by ^1H NMR. The isomer ratios in equilibrium were apparently different between the thermal and photochemical processes. Similar studies with diruthenium homologues, (μ_2:η^3:η^5-guaiazulene)$Ru_2(CO)_5$ (**2a,b**), were also undertaken in order to determine the differences in reactivity and selectivities of the haptotropic interconversion from the diiron complexes. Thermal and photochemical ligand substitution reactions of **1a,b** by PEt_3[4a] were also reexamined. The results suggest that the haptotropic rearrangement proceeded both thermally and photochemically by different mechanisms (Scheme 1).

Results and Discussion

Assignment of the NMR Spectra. Preparation of **1a,b** was carried out according to the procedures reported by Cotton[4a] and Wilkinson.[4b] Since no detailed description was given on the ^1H NMR spectra of these compounds in the literature,[4] we first carried out the assignment of the peaks derived from the guaiazulene

[⊗] Abstract published in *Advance ACS Abstracts,* August 1, 1994.

(1) Mann, B. E. In *Comprehensive Organometallic Chemistry*; eds. Wilkinson, G., Stone, F. G. A., Abel, E. W., Eds.; Pergamon: Oxford, U.K., 1982; Vol. 3, p 89. Deganello, G. *Transition Metal Complexes of Cyclic Polyolefins*; Academic Press: New York, 1982.

(2) (a) Albright, T. A.; Hofmann, P.; Hoffmann, R.; Lillya, C. P.; Dobosh, P. A. *J. Am. Chem. Soc.* **1983**, *105*, 3396. (b) Rerek, M. E.; Basolo, F. *Organometallics* **1984**, *3*, 647. (c) Nakasuji, K.; Yamaguchi, M.; Murata, I.; Nakanishi, H. *J. Am. Chem. Soc.* **1986**, *108*, 325. (d) Kirss, R. U.; Treichel, P. M. *Ibid.* **1986**, *108*, 853. (e) Decken, A.; Britten, J. F.; McGlinchey, M. J. *Ibid.* **1993**, *115*, 7275 and references cited therein.

(3) Nagashima, H.; Fukahori, T.; Itoh, K. *J. Chem. Soc., Chem. Commun.* **1991**, 786.

(4) (a) Cotton, F. A.; Hanson, B. E.; Kolb, J. R.; Lahuerta, P.; Stanley, G. G.; Stults, B. R.; White, A. J. *J. Am. Chem. Soc.* **1977**, *99*, 3673. (b) Burton, R.; Pratt, L.; Wilkinson, G. *J. Chem. Soc.* **1960**, 4290.

0276-7333/94/2313-3427$04.50/0 © 1994 American Chemical Society

Scheme 1

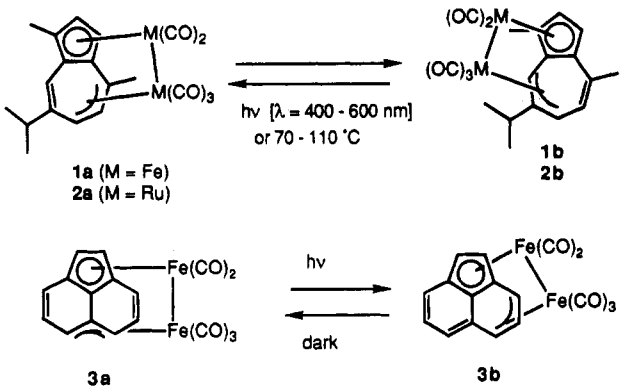

ligand by careful $^1H\{^1H\}$ decoupling NOE experiments. The results are summarized in Table 1. In these guaiazulene complexes, four vinyl protons bonded to the iron atoms generally appeared at 2.3–5.0 ppm, showing a significantly higher field shift of the signals compared with those of uncoordinated guaiazulene. In contrast, the one remaining proton was observed within the region of usual olefinic protons at 4.3–5.1 ppm. These results suggest that the solid-state structures reported for **1a,b**,[4a] in which the guaiazulene ligand was bound to two iron atoms with Fe(1)↔cyclopentadienyl and Fe(2)↔π-allyl coordination modes, respectively, are maintained in solution. Similar assignments of ^1H NMR spectra of **2a,b** are also shown in Table 1.

Interconversion Studies. The thermal haptotropic rearrangement between **1a** and **1b** occurred at higher than 70 °C in toluene-d_8. In order to avoid the photochemical rearrangement described below, solutions of **1a,b** were carefully protected from the light. Reaction profiles at 70–105 °C monitored by ^1H NMR are shown in Figure 1. The reactions were essentially reversible. The equilibrium constants (K_{eq} = [**1b**]/[**1a**]) measured by ^1H NMR were 0.82 ± 0.1 at 70, 80, 90, and 100 °C, which indicates that **1a** is more stable than **1b** by 0.1 kcal/mol. The interconversion between **1a** and **1b** was investigated further in kinetic studies. Two series of experiments starting from either pure **1a** or pure **1b** were carried out at four different temperatures. The data were treated in terms of reversible-first-order kinetics, and the rate constants [$(k_1)_{obs}$ observed in the reaction from **1a** and $(k_{-1})_{obs}$ observed in the reaction from **1b** (s^{-1})] were determined as follows: $(k_1)_{obs}$ = (1.03 ± 0.02) × 10^{-5} (355 K), (3.11 ± 0.03) × 10^{-5} (367 K), (5.32 ± 0.03) × 10^{-5} (373 K), (7.90 ± 0.10) × 10^{-5} (378 K); $(k_{-1})_{obs}$ = (1.45 ± 0.03) × 10^{-5} (355 K), (4.24 ± 0.06) × 10^{-5} (367 K), (7.87 ± 0.14) × 10^{-5} (373 K), (1.30 ± 0.04) × 10^{-4} (378 K). The rate constants can be alternatively calculated from these observed values using the equation $K_{eq} = k_1/k_{-1}$ and were consistent with the observed data within experimental errors. The values of the activation parameters were identical in both of the reaction pathways, **1a** to **1b** and **1b** to **1a** [$\Delta G^{\ddagger}_{373}$ = 28 ± 1 kcal/mol, $\Delta H^{\ddagger}_{373}$ = 23 ± 2 kcal/mol, $\Delta S^{\ddagger}_{373}$ = −15 ± 5 cal/(mol·deg)]. Details on the kinetics are summarized in the supplementary materials.

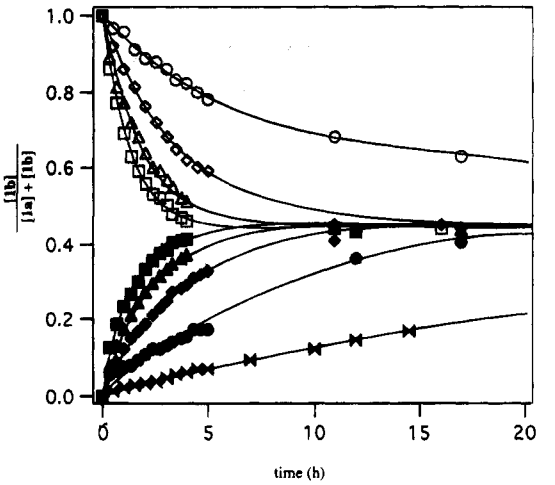

Figure 1. Reaction profiles for the thermal interconversion between **1a** and **1b**: **1a** → **1b**, 343 K (fused triangles), 355 K (●), 367 K (◆), 373 K (▲), 378 K (■); **1b** → **1a**, 355 K (○), 367 K (◇), 373 K (△), 378 K (□).

The haptotropic rearrangement between **1a** and **1b** did not take place at room temperature as long as the solution was protected from the light. However, exposure of the solution to the visible light (λ = 400, 500, or 600 nm; controlled by UV-cutoff filters) resulted in facile interconversion between them. The reaction profiles are illustrated in Figure 2. The light with λ > 680 nm barely induced the rearrangement. UV–visible spectra of **1a,b** indicate that a broad absorption around 500 nm

Table 1. ^1H NMR Spectra of 1a,b and 2a,b (δ, ppm)[a]

	1a	1b	2a	2b
H1	3.07 (d), J = 2.4 Hz	4.44 (d), J = 2.4 Hz	3.13 (d), J = 2.4 Hz	4.95 (d), J = 2.4 Hz
H2	4.29 (d), J = 2.4 Hz	4.18 (d), J = 2.4 Hz	5.06 (d), J = 2.4 Hz	4.90 (d), = 2.4 Hz
H3	4.58 (d), J = 8.3 Hz	4.95 (dd), J = 1.5, 8.8 Hz	4.70 (d), J = 8.8 Hz	4.64 (dd), J = 1.5, 8.8 Hz
H4	2.85 (dd), J = 2.0, 8.8 Hz	2.89 (dd), J = 2.0, 8.8 Hz	2.98 (dd), J = 1.5, 8.8 Hz	3.04 (dd), J = 2.0, 8.8 Hz
H5	5.01 (d), J = 2.0 Hz	4.35 (d), J = 2.0 Hz	4.99 (d), J = 2.0 Hz	4.37 (d), J = 2.0 Hz
Me1	1.51 (s)	1.18 (d), J = 1.5 Hz	1.45 (s)	1.17 (d), J = 1.5 Hz
Me2	1.60 (s)	1.07 (s)	1.85 (s)	0.99 (s)
*i*Pr	0.81 (d), J = 6.8 Hz, 0.83 (d), J = 6.8 Hz, 1.87 (sept), J = 6.8 Hz	1.10 (d), J = 6.8 Hz, 1.12 (d), J = 6.8 Hz, 2.29 (sept), J = 6.8 Hz	0.75 (d), J = 6.8 Hz, 0.79 (d), J = 6.8 Hz, 1.79 (sept), J = 6.8 Hz	1.10 (d), J = 6.8 Hz, 1.12 (d), J = 6.8 Hz, 2.39 (sept), J = 6.8 Hz

[a] All spectra were taken in C_6D_6 at room temperature. Assignment was unequivocally carried out by the $^1H\{^1H\}$ decoupling technique and NOE measurement. Atoms are labeled as follows:

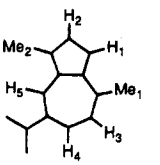

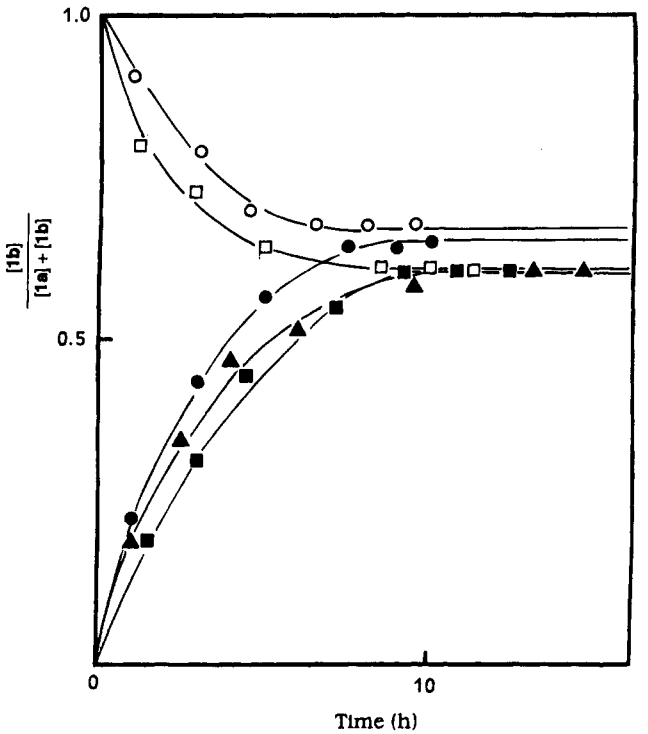

Figure 2. Reaction profiles for the photochemical interconversion between **1a** and **1b**: **1a** → **1b**, λ = 400 nm (▲), 500 nm (●), and 600 nm (■); **1b** → **1a**, λ = 500 nm (○) and 600 nm (□).

is likely to induce the photochemical haptotropic rearrangement. After irradiation for 4–5 h, the ratio of **1a** to **1b** reached 35:65 and was independent on the wavelength. *Of importance is that the product ratio at the photostatic states (35:65) is different from the thermal equilibrium ratio (55:45) described above. In other words, the product ratios can be controlled either by visible irradiation or by heating in the dark, though the difference in the isomer ratios was not significantly large between the two processes.*

The haptotropic rearrangement of diruthenium analogues, (μ^2:η^3:η^5-guaiazulene)$Ru_2(CO)_5$ (**2a,b**), also occurred by both thermal and photochemical processes; however, the equilibrium ratios between the two processes were similar. The thermal reactions proceeded at lower temperature than those of the diiron analogues as briefly noted in the literature.[4a] From either a 1:4 or a 4:1 mixture of **2a,b**, a 55:45 mixture of them was obtained at room temperature within 3 h. Photochemical studies of **2a,b** at −40 °C with visible light (λ = 500 nm), at which the thermal process did not occur, revealed that the ratios between **2a** and **2b** reached 55:45 after several hours. Rapid thermal equilibrium between **2a** and **2b** prevented detailed studies.

Thermal and Photochemical Ligand Substitution of 1a,b To Form 4 and 5. Cotton and co-workers reported that photochemical ligand substitution of **1a,b** by PEt_3 resulted in the formation of a monophosphine complex **4**,[4a] which was not accomplished by a thermal process. Reexamination of these thermal and photochemical ligand replacement reactions provided the following interesting findings to indicate that they are governed by different mechanisms.

The thermal ligand substitution with 0.7 equiv of PEt_3 in toluene-d_8 at 100 °C in the dark revealed that the ligand substitution ($t_{1/4}$ > 2 days) was preceded by the

Scheme 2

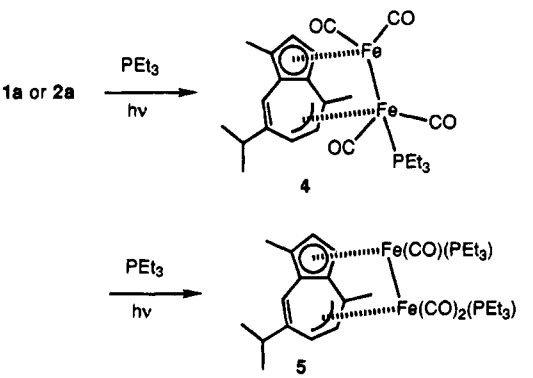

Table 2. ^{1}H NMR Data for 4 and 5 (δ, ppm)[a]

	4	5
H1	3.24 (d), J = 2.4 Hz	3.69 (dd), J = 2.5 Hz, J_{PH} = 5.0 Hz
H2	4.64 (d), J = 2.4 Hz	4.43 (dd), J = 2.5 Hz, J_{PH} = 5.0 Hz
H3	4.24 (dd), J_{PH} = 5.7 Hz, J = 8.8 Hz	4.16 (dd), J_{PH} = 5.9 Hz, J = 8.8 Hz
H4	2.28 (ddd), J = 1.2, 8.8 Hz, J_{PH} = 5.7 Hz	2.58 (ddd), J = 1.5, 8.8 Hz, J_{PH} = 5.9 Hz
H5	5.10 (d), J = 1.2 Hz	5.26 (d), J = 1.5 Hz
Me1	1.85 (s)	1.78 (s)
Me2	1.87 (s)	1.98 (s)
*i*Pr	1.01 (d), J = 6.8 Hz, 1.02 (d), J = 6.8 Hz, 2.09 (sept), J = 6.8 Hz	1.16 (d), J = 6.8 Hz 2.25 (sept), J = 6.8 Hz
PEt_3	0.79 (dt), J = 6.8, 7.5 Hz, 1.02 (dq), J = 6.8, 8.8 Hz	1.04–0.89, 1.46–1.58, 1.64–1.77 (m)

[a] All spectra were taken in C_6D_6 at room temperature. Assignment was unequivocally carried out by the ^{1}H{^{1}H} decoupling technique and NOE measurement. Atom labeling is shown in Table 1.

haptotropic interconversion between **1a** and **1b** ($t_{1/2}$ = 2 h). Neither the rate nor the equilibrium ratio of the haptotropic interconversion between **1a** and **1b** in the presence of PEt_3 differed from that in its absence. Prolonged heating resulted in the formation of **4**, during which no other peak assignable to either the reaction intermediates or a diphosphine complex **5** (*vide infra*) was observed[5,6] (Scheme 2).

In contrast, either UV or visible (λ = 500 nm) irradiation of a benzene-d_6 solution of **1a** or **1b** in the presence of PEt_3 resulted in efficient substitution of the CO ligand by PEt_3 to form two products, **4** and **5**.[7] Their NMR assignments are summarized in Table 2. ^{1}H NMR studies of the photochemical ligand substitution revealed the following. First, the reactions with 0.7 equiv of PEt_3 gave **4** as the major product, whereas, in the presence of 5 equiv of PEt_3, **5** was mainly formed. The formation of **5** from **1a** or **1b** is likely to be stepwise, because **4** appeared at the initial stage of the reaction and then diminished. Second, the haptotropic rearrangement between **1a** and **1b** was not observed in the presence of PEt_3, in sharp contrast to the fact that the rearrangement preceded the ligand substitution in the

(5) Attempted kinetic studies with 5 equiv of PEt_3 failed due to extensive line broadening of the NMR signals on heating, during which the starting materials were probably decomposed.

(6) A slight difference was observed in the reaction profiles between the reactions from **1a** and **1b**; the slow formation of **4** was observed even at the initial stage of the reaction from **1a**, whereas an induction period was recognized in the reaction from **1b**. During the induction period, the haptotropic rearrangement to form **1a** was observed, which may suggest that **4** was not formed directly from **1b** but was produced through **1a**.

Scheme 3

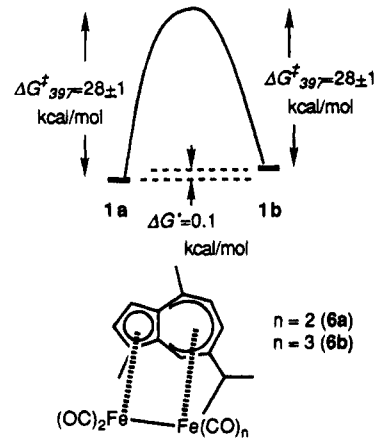

thermal process. This result is curious because the rate of the formation of **4** was similar to that of the haptotropic interconversion ($t_{1/2}$ = 1 h). A reasonable explanation is that the photo-activated species from **1a** or **1b** with PEt_3 is reactive enough toward the ligand substitution by PEt_3 to suppress the haptotropic rearrangement.

Mechanism. The energy diagram of the thermal interconversion between **1a** and **1b** is illustrated in Scheme 3. The thermal haptotropic rearrangement of monometallic species on the polyene or aromatic ligands was extensively studied theoretically and experimentally.[2] Albright and co-workers calculated the intramolecular migration of the organometallic fragments across the surfaces of polycyclic systems, which can be rationalized in terms of the interactions between the frontier orbitals of the ML_n moiety and of the π-system.[2a] Kinetic studies on slipping of $Mn(CO)_3$ species from the six-membered ring to the five-membered one in several fluorenylmanganese complexes and migration of the $Cr(CO)_3$ unit from one ring to another in several naphthalene–chromium complexes were carried out by Basolo[2b] and Treichel,[2d] respectively, revealing that experimental values of $\Delta H^{\ddagger}$ (27–34 kcal/mol) for both systems compare quite favorably with the predicted values of the activation energies by theory.[2a] Small values of $\Delta S^{\ddagger}$ (−1 to 3 cal/(mol·deg)) were also obtained for these processes, supporting the intramolecular rearrangement. A possible reaction pathway for the interconversion between **1a** and **1b** is intramolecular slippage of the $Fe_2(CO)_5$ species on conjugate π-electrons in the guaiazulene ligand similar to those proposed for the rearrangement of naphthalene–chromium complexes and fluorenylmanganese carbonyls.[2a,b,d] The experimentally obtained activation energy ($\Delta H^{\ddagger}$) is 23 ± 1 kcal/mol. The $\Delta S^{\ddagger}$ for the interconversion for the haptotropic rearrangement between **1a** and **1b** was negative (−15 ± 5 cal/(mol·deg)) in contrast to the negligible values observed in the rearrangement of naphthalene–chromium complexes and fluorenylmanganese compounds. Although it should be taken into account that our $\Delta S^{\ddagger}$ value was determined by the rate constants measured in a small temperature range (20 °C) and may contain the larger experimental error, it is worthwhile to point out that there is a possibility that intramolecular association of the uncoordinated carbon–carbon double bond in **1a,b** affords an activated complex **6b** with a total of 38-valence electrons in the transition states. An alternative pathway for the thermal haptotropic rearrangement is that dissociation of a CO ligand in **1a,b** accompanied by the intramolecular coordination of the uncoordinated carbon–carbon double bond gives (μ_2:η^5:η^5-guaiazulene)$Fe_2(CO)_4$ (**6a**), the reaction of which with CO induces the haptotropic rearrangement. The thermal replacement of CO ligands in metal carbonyls by olefins is a common process in organometallic chemistry.[8] However, the very slow reaction of **1a,b** with PEt_3 in the thermal process described above is likely to exclude this reaction pathway. Cotton and co-workers proposed **6a** as an intermediate, which can easily react with PEt_3, in the photochemical formation of **4**.[4a]

Scheme 4

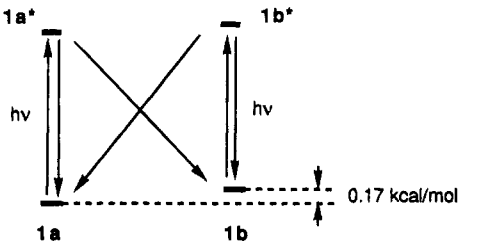

The reaction scheme for the photochemical interconversion between **1a** and **1b** is illustrated in Scheme 4. Since the reaction pathway of **1a** → **1a*** → **1b** is more efficient than that of **1b** → **1b*** → **1a**, the isomer ratio at the photostatic states is different from that observed in the thermal reaction. It is known that photoirradiation of bimetallic metal carbonyls provides dissociation of the CO ligand and cleavage of the metal–metal bond; for example, photochemical processes of $[CpFe(CO)_2]_2$ by time-resolved IR studies revealed that a number of short-lived intermediates derived from the

(7) ^1H, ^{13}C, and ^{31}P NMR spectra of **4** revealed that the crystal structure reported by Cotton[4a] was maintained in solution. The diphosphine complex **5** was reported as "a black unidentified product" in the literature.[4a] Characterization of **5** was done by comparison of its NMR spectra with those of **4**. The $^{31}P\{^1H\}$ NMR spectrum of **4** showed a singlet at δ 57.13 ppm, whereas **5** showed two ^{31}P resonances at δ 52.95 and 55.22 ppm as singlets, in which no ^{31}P–^{31}P coupling was observed. The ^1H NMR spectrum of **4** showed that C–H signals bound to the $Fe(CO)_2(PEt_3)$ species (H_3 and H_4) split into doublets (J = 5.7 Hz) due to the coupling with the ^{31}P nucleus; however, no ^1H–^{31}P coupling was observed for those bonded to the $Fe(CO)_2$ moiety (H_1 and H_2). In contrast, that of **5** showed all of the protons bonded to the Fe atoms (H_1–H_4) split into doublets by the coupling with the ^{31}P nucleus. Four ^{13}C signals derived from the CO ligands were observed for **4**, two of which split into doublets due to the coupling with ^{31}P nuclei. In contrast, **5** contained three ^{13}C resonances derived from the CO ligands, two of which were coupled with the ^{31}P nuclei. These NMR data suggest that both of the iron atoms in **5** are bonded to PEt_3, being consistent with (μ_2:η^3:η^5-guaiazulene)Fe(CO)(PEt_3)$Fe(CO)_2(PEt_3)$ (**5**), which was the result of the replacement of one CO ligand on each Fe atom of **1a,b** by PEt_3. It is possible that two isomers exist in **5** (**5a,b**)

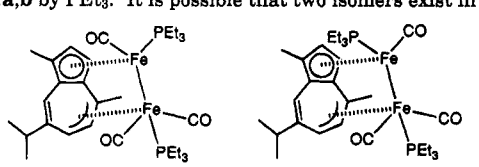

5a **5b**

though only a single isomer of **5** was formed. Final determination of the structure has not been achieved due to the difficulty in making a single crystal of **5** for X-ray analysis; however, the isomer **5a** would be preferable to **5b** to minimize steric repulsion between the methyl group on the guaiazulene ligand and the ethyl groups on PEt_3.

(8) For example, $Fe(CO)_5$ reacted with norbornadiene to form (η^4-norbornadiene)$Fe(CO)_3$: Pettit, R. *J. Am. Chem. Soc.* **1959**, *81*, 1266.

Scheme 5

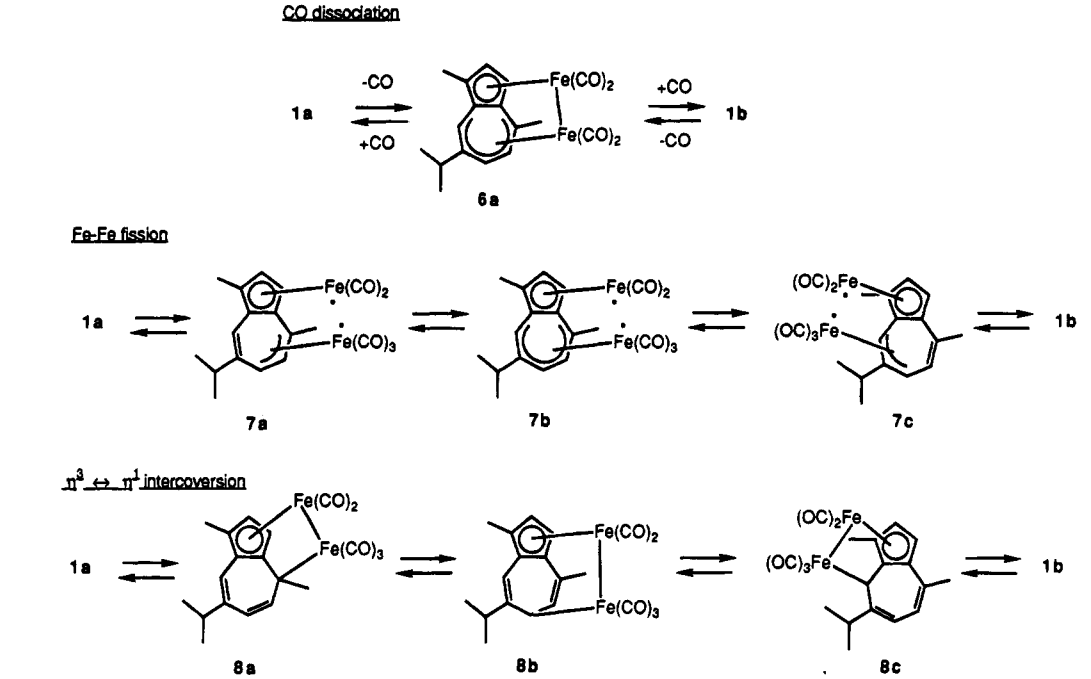

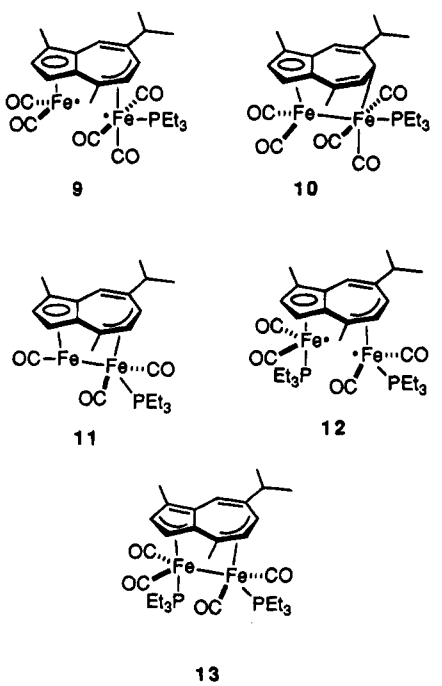

Figure 3.

CO dissociation or the fission of the Fe—Fe bond were produced by UV or visible photolysis.[9,10] It was also pointed out that η^5 to η^3 interconversion of the Cp ring was involved in the photochemical processes of $[CpFe(CO)_2]_2$.[10] Thus, photolysis of (μ_2:η^3:η^5-guaiazulene)$Fe_2(CO)_5$ provides three types of possible intermediates: **6a** by photochemical dissociation of the CO ligand, **7a–c** derived from the Fe—Fe bond fission, and **8a–c** resulted from the η^3 to η^1 conversion of the $Fe(CO)_3$ species on the seven-membered ring of the guaiazulene ligand. As shown in Scheme 5, the haptotropic rearrangement can occur through any of these three intermediate types. The reaction of **6a** with CO affords a mixture of **1a,b**. Since many studies suggest that 17-electron metalloradical species such as $\cdot Mn(CO)_5$ are active toward the associative ligand substitution,[11] association of the uncoordinated carbon—carbon double bond in **7a,c** results in the reversible formation of **7b**, by way of which **7a,c** are mutually interconverted. The $\eta^3 \leftrightarrow \eta^1$ conversion of **1a** provides intermediates **8a,b**, and that of **1b** provides **8b,c**. Equilibrium among **8a** ↔ **1a** ↔ **8b** ↔ **1b** ↔ **8c** accomplishes the interconversion between **1a** and **1b**. As described above, irradiation of **1a,b** in the presence of PEt_3 resulted in exclusive formation of **4** or **5**, which suggests that the photo-activated species can easily react with PEt_3. The intermediates **6a**, **7a–c**, and **8a–c** can react with PEt_3 to result in the ligand substitution reactions to form **4**. Substitution of a coordinated carbon—carbon double bond in **6a** by PEt_3 on the iron center provides **4**. Both the metalloradical intermediate **7a** and the μ_2:η^5:η^1-intermediate **8a** undergo facile associative substitution of a CO group by PEt_3 on the iron center via the intermediates **9** and **10**, respectively (Figure 3). Although determination of actual photo-activated species should await further studies including direct spectroscopic observation, the photochemical haptotropic rearrangement of **1a,b** is likely to involve either the CO dissociation, the metal—metal bond cleavage, or the hapticity change.[12]

Conclusion

As described in our previous paper, the diiron acenaphthylene complexes show characteristic behavior like an "organometallic photoswitch", in which the coordination site of the diiron species is changed either on irradiation or protection from the light.[3] The present results revealed that diiron or diruthenium guaiazulene com-

(9) For reviews: Meyer, T. J.; Casper, J. V. *Chem. Rev.* **1985**, *85*, 187. Poliakoff, M.; Weitz, E. *Adv. Organomet. Chem.* **1986**, *25*, 277.

(10) Dixon, A. J.; George, M. W.; Hughes, C.; Poliakoff, M.; Turner, J. J. *J. Am. Chem. Soc.* **1992**, *114*, 1719. Zhang, S.; Brown, T. L. *Ibid.* **1993**, *115*, 1779.

(11) For example: Kochi, J. K. In *Paramagnetic Organometallic Species in Activation/Selectivity, Catalysis*; Channon, M., Julliard, M., Poit, J. C., Eds.; NATO ASI Series C; Plenum: New York, 1989; Vol. 257, p 149.

Table 3. ^{13}C NMR Spectra of 1a,b, 3, and 4 (Guaiazulene Region; δ, ppm)[a]

	1a	1b[b]	4	5
C1	72.92	82.06 (81.96)	71.66	71.45
C2	82.06	81.62 (81.56)	81.31	78.45
C3	83.16	*c* (128.04)	82.85	81.07
C4	53.90	58.38 (58.16)	50.55	52.70
C5	109.60	54.03 (53.89)	108.11	107.83
Me1	23.93	27.11 (27.27)	23.26	23.68
Me2	11.74	10.29 (10.63)	12.16	12.51
*i*Pr (Me)	21.36, 22.37	18.90 (19.06), 20.21 (18.40)	22.09, 22.71	22.73, 23.04
*i*Pr (CH)	37.96	37.43 (37.33)	38.32	38.58
quartarnary carbon	73.84, 79.95, 83.90, 101.91, 150.49	71.87 (71.47), 85.40 (85.30), 93.35 (93.47), 108.32 (108.41), 124.49 (124.80)	69.50, 75.69, 82.67, 99.85, 151.10	65.72, 74.63, 76.79, 92.62, 147.25
PEt_3 (CH_2)			19.10 (d) (J_{PC} = 25.0 Hz)	19.25 (d) (J_{PC} = 21.4 Hz), 21.65 (d), (J_{PC} = 21.4 Hz)
PEt_3 (Me)			7.57 (s)	7.79 (s), 8.50 (s)

[a] All spectra were measured in C_6D_6 at room temperature unless otherwise noted. Signals of the CO region are descirbed in the Experimental Section. [b] Figures in parentheses are the chemical shifts observed in $CDCl_3$. [c] The peak was coincidentally identical to those of C_6D_6. Atoms are labeled as follows:

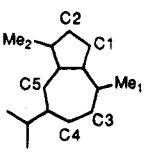

plexes, **1a,b** or **2a,b**, also underwent the haptotropic interconversion between the two haptotropic isomers either thermally or photochemically. In the case of the diiron complexes, the isomer ratios under irradiation were different from those in the dark at 70–105 °C. Thus, **1a,b** are another example of the photoswitch-like behavior, though the selectivity of the reaction is less significant than that for the diiron acenaphthylene complexes. These results indicate that the photodirected switching of the coordination site would be generally observed in other dimetallic carbonyl compounds bound to polyaromatic or polyolefin ligands having dual haptotropic isomers, the exploration of which is in progress. A mechanism involving the slippage of $Fe_2(CO)_5$ species on the conjugate π-electrons in the guaiazulene ligand was proposed for the thermal haptotropic rearrangement, whereas those via the CO dissociation, the metal–metal bond cleavage, or the hapticity change were proposed for the photochemical interconversion. These mechanisms will help in the exploration of other photoswitch molecules.

Experimental Section

General Methods. NMR spectra were taken with a JEOL GX-270 spectrometer in C_6D_6 unless otherwise noted. Chemical shifts were recorded in ppm from the internal standard (^1H, ^{13}C = solvent; ^{31}P = H_3PO_4), and the coupling constant was done in Hz. IR spectra were recorded on a JASCO IR 3A spectrometer and measured in cm^{-1}. All experiments were carried out under an inert-gas atmosphere using standard Schlenk techniques. ^1H NMR spectra of **1a,b**, **2a,b**, **4**, and **5** are summarized in Tables 1 and 2. Assignment of ^{13}C NMR spectra of the guaiazulene ligand in **1a,b**, **4**, and **5** was done by the $^{13}C\{^1H\}$-selective decoupling method as summarized in Table 3.

Preparation and Separation of 1a,b. Diiron compounds **1a,b** were prepared by Cotton's method.[4a] Separation of the haptotropic isomers **1a,b** was carried out by an Al_2O_3 column (activity II–III, Merck 1097). The purified samples were subjected to recrystallization from pentane at −20 °C before use. Fluxional behavior was observed with ^{13}C NMR of the CO ligands in **1a** or **1b**. At room temperature in C_6D_6, three peaks at δ 214.3, 217.0, and 220.5 in a ratio of 1:3:1 were observed for **1a**, whereas one peak at δ 218.6 ppm was noted for **1b**. These signals correspond to the data around 0 °C in a 95:5 mixture of acetone-d_6 and CS_2 reported in the literature.[4a]

1a: Mp 94–95 °C (lit.[4b] mp 97–99 °C). **1b**: Mp 108–109 °C (lit.[4b] 110–111 °C).

Preparation and Separation of 2a,b. Diruthenium complexes **2a,b** were prepared similarly. Compared with the diiron analogues, the yields of the diruthenium compounds were low (around 25% based on $Ru_3(CO)_{12}$) due to the formation of trinuclear and tetranuclear clusters bound to guaiazulene.[13] The chromatography with Al_2O_3 (CH_2Cl_2–hexane) was carried out at −70 °C, and fractions were kept cool with an ice bath and protected from visible light during collection and concentration. A 1:4 or a 4:1 mixture of **2a,b**, which allowed the unequivocal assignments of the ^1H NMR spectra, was subjected to the interconversion studies without further purification.

Preparation of Phosphine Compounds 4 and 5 from 1a. Substitution of one or two of the CO ligands in **1a** was made under UV irradiation with a 500-W high-pressure Hg lamp. A mixture of **1a** (80 mg, 0.178 mmol) and PEt_3 (26.2 μL, 0.178 mmol) in benzene (9.6 mL) was irradiated at room temperature for 12 h to give **4** (28 mg, 29% yield) with a recovery of **1a** (21 mg) (74% conversion, 39% yield). Treatment of **1a** (80 mg, 0.178 mmol) with excess PEt_3 (131 μL, 0.89 mmol) under UV irradiation for 10 h gave **4** (11 mg, 11%) and **5** (74 mg, 66%) with a recovery of **1a** (10 mg, 13%) (87% conversion, 76% yield). In both cases, the reaction mixture was concentrated and the residue obtained was purified with

(12) If we assume that the photochemical ligand substitution by PEt_3 proceeds through intermediates similar to those in the photochemical haptotropic rearrangement, the mechanism should also explain facile formation of the diphosphine product **5** in the photochemical reaction of **1a** or **1b** with excess PEt_3. This assumption provides a possibility that the reaction pathways involving the Fe–Fe bond cleavage or the hapticity change are more apt to be the mechanisms for the photochemical haptotropic rearrangement than that via the CO dissociation. In the mechanism through **6a**, the intramolecular coordination of the uncoordinated C=C bond in **1a** or **1b** is essential for the dissociation of CO from **4** to form the intermediate **6a**. In sharp contrast, there is no appropriate C=C double bond to stabilize an intermediate such as **11** for the CO dissociation at another iron atom. Thus, the mechanism involving the Fe–Fe bond cleavage or the $\eta^5 \leftrightarrow \eta^3$ conversion can explain the facile disubstitution to form **5** through an intermediate such as **12** or **13** (Figure 3).

(13) The structures of the products were determined by X-ray analysis: Nagashima, H.; Nobata, M.; Suzuki, A.; Aoki, K.; Itoh, K. Unpublished results. Homologous compounds: Churchill, M. R. *Prog. Inorg. Chem.* **1970**, *9*, 2239.

a Al_2O_3 column at −78 °C. Elution with hexane gave three bands; the first blue, the second red, and the third brown band corresponded to guaiazulene, **4**, and **5**, respectively.

4: Mp 92−93 °C (lit. mp 93−94 °C);[4a] $^{31}P\{^1H\}$ NMR δ 57.13 (s); ^{13}C NMR (CO region) δ 215.8 (d, J_{PC} = 20.0 Hz), 222.3 (s), 226.6 (s), 234.8 (d, J_{PC} = 15.4 Hz) [lit.[4a,14] ^{13}C NMR in acetone-d_6−CS_2: 212.4 (d), 217.2 (s), 222.3 (s), 234.7 (d)]; IR (KBr) 1985 (s), 1930 (s), 1884 (sh) (lit.[4a] IR 1990, 1938). **5**: Mp 95−98 °C (dec); $^{31}P\{^1H\}$ NMR δ 52.95 (s), 55.22 (s); ^{13}C NMR (CO region) δ 221.8 (d, J_{PC} = 22.6 Hz), 224.3 (d, J_{PC} = 27.6 Hz), 234.8 (br s); IR (KBr) 2027 (m), 1978 (s), 1936 (m), 1926 (m). Anal. Calcd for $C_{30}H_{48}O_3Fe_2P_2$: C, 57.14; H, 7.62. Found: C, 57.77, H, 7.62.

^{1}H NMR Studies for the Haptotropic Interconversion between 1a and 1b or 2a and 2b. Thermal interconversion between **1a** and **1b** or **2a** and **2b** was monitored in toluene-d_8 (0.033 M), whereas photochemical studies were done in benzene-d_6 (0.0033 M). The NMR samples were carefully degassed several times and sealed in a vacuum. The heated or irradiated samples were quenched periodically by cooling them at −78 °C and were kept cold until the NMR measurement. The thermal reactions to determine the equilibrium constants were undertaken in an oil bath, the temperature at which was carefully controlled by a thermocouple (70, 80, 90, and 100 ± 1 °C). Visible irradiation was done by a 500-W Xe lamp through a Toshiba UV cut-off filter (λ = 400, 500, 600 nm) and a water filter. A 500-W high-pressure Hg lamp was used for the UV irradiation.

Kinetic Studies. The reactions were conducted in sealed tubes, and the concentration of the product was followed by variable-temperature ^{1}H NMR spectroscopy. Two series of experiments starting from either pure **1a** or pure **1b** were carried out at four different temperatures (355, 367, 373, 378 K). The data were treated in terms of reversible-first-order kinetics; plots of (x_e/a) ln $[x_e/(x_e - x)]$, where x_e is the concentration of the product in equilibrium, a is the initial concentration of the reactant, and x is the concentration of the product at time t, vs time resulted in straight lines ($r > 0.99$). The rate constants $[(k_1)_{obs}$ and $(k_{-1})_{obs}]$ were extracted as the slopes of these lines. The rate constants were alternatively calculated from these observed values according to the equation $K_{eq} = k_1/k_{-1}$ and were consistent with the observed data within the experimental errors. Plots of logarithmic function of the rate constants vs reciprocal of temperature gave typical Arrhenius plots, from which the activation parameters at 373 K were determined. Details are given in the supplementary data.

(14) The chemical shifts were recorded from CS_2 in the literature.

Acknowledgment. Financial support from the Ministry of Education, Science, and Culture of the Japanese government (Grant-in-Aid for Priority Areas, Nos. 04241215 and 05225215) and helpful discussions by Professor Sanshiro Komiya (Tokyo University of Agriculture and Technology) are acknowledged.

Supplementary Material Available: Text, tables, and figures providing details on the kinetic studies and NOE experiments for the assignment of **1a**,**b** (12 pages). Ordering information is given on any current masthead page.

OM930828C